

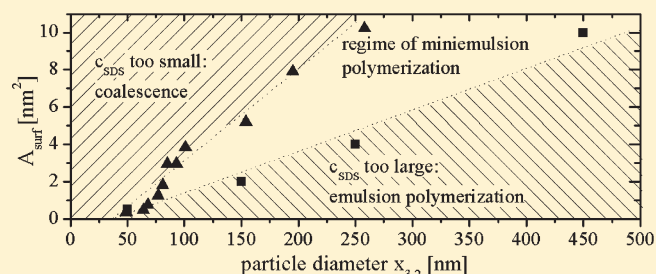
Surfactant Concentration Regime in Miniemulsion Polymerization for the Formation of MMA Nanodroplets by High-Pressure Homogenization

Lena L. Hecht,^{*,†} Caroline Wagner,[‡] Katharina Landfester,[‡] and Heike P. Schuchmann[†]

[†]Karlsruhe Institute of Technology (KIT), Institute for Process Engineering in Life Science, Section I: Food Process Engineering, Karlsruhe, Germany

[‡]Max-Planck-Institute for Polymer Research, Mainz, Germany

ABSTRACT: This article focuses on the adequate surfactant concentration regime in which MMA droplets are stabilized sufficiently against coalescence during high-pressure homogenization but still no diffusion processes from droplets to micelles take place in the polymerization. Monomer miniemulsions with different surfactant concentrations were prepared with different energy inputs. Emulsions result that depend either on the surfactant concentration or on the energy input of the homogenization process. For both cases, the occupancy of the interface is compared as a function of the droplet size. It is shown that the surfactant concentration needed for the stabilization of a specified interface area decreases with increasing droplet size. For the dependence of droplet size on the energy input, it is shown that more surfactant can be applied before emulsion polymerization starts, but the applicable surfactant concentration is lower than the cmc and also depends on droplet size.



1. INTRODUCTION: MOTIVATION AND PRINCIPLE PROCESS SCHEME

Miniemulsion polymerization is an advantageous process for the encapsulation of insoluble components into a polymer matrix.^{1,2} This has been of ongoing interest in academics and industry in the last few years. Many different applications for hybrid nanoparticles with encapsulated components have been developed, for example, in paints,^{3,4} where the polymer coating prevents the particles from agglomerating, thus improving the color intensity. Furthermore, nanocapsules allow control over the release of encapsulated components,^{5,6} enhancing the performance of catalysts,⁷ depressing toxic shock,⁸ and reducing drug degradation⁹ in medical applications.

For the production of hybrid nanoparticles, a two-stage process is described in the literature,^{10–13} with the emulsification of a nanoparticle-in-monomer suspension as the first process step and the polymerization of the filled submicrometer-sized monomer droplets by miniemulsion polymerization as the second process step. The polymerization takes place within the droplets, which in fact act as “nanoreactors”. For this, nanoparticles have to be homogeneously dispersed in the monomer, which requires lipophilic surface functionalization. The nanoparticle-in-monomer suspension is then emulsified in an aqueous phase and homogenized to target droplet sizes in the range of $d < 500$ nm. Controlling this process step is essential, as in the following miniemulsion polymerization droplets are transformed directly into particles, ideally in a 1:1 copy. Thus, the droplet size distribution as adjusted in homogenization directly determines the final product properties.

Miniemulsion droplets are stabilized by a surfactant against coalescence and by an osmotic pressure agent against Ostwald ripening.¹⁴ To ensure that the identity of the droplets will be kept during miniemulsion polymerization, micellar nucleation as typically found in emulsion polymerization has to be avoided.¹⁵ Therefore, the surfactant concentration in the continuous phase has to be below the critical micelle concentration (cmc) after the emulsification step.¹⁶ In addition to micellar and droplet nucleation, homogeneous nucleation can happen at surfactant concentrations below the cmc when monomer molecules that are initiated in the bulk phase can grow to oligomers and precipitate.¹⁷ If the surfactant is used in the right concentration range, then a 1:1 copy of droplets to particles is possible.¹⁵ All nucleation mechanisms can be observed for water-soluble initiators but are also valid for oil-soluble initiators because the radicals exit the droplet and radicals in the aqueous phase contribute significantly to the polymerization rate.¹⁸ The consequence of micellar and homogeneous nucleation is a mixture of unfilled polymer particles and incompletely covered core particles and is not desirable in the production of polymeric nanoparticles with encapsulated components.

Such particles in the size range well below $1 \mu\text{m}$ require a certain energy-input level in the homogenization step.¹⁹ Technical processes known to disrupt droplets are rotor-stator systems (RS), high-pressure homogenization (HPH), and ultrasonication (US).²⁰

Received: November 10, 2010

Revised: January 6, 2011

Published: February 11, 2011



All processes have in common that the rheological behavior of the droplets and the continuous phase strongly influences droplet deformation and breakup.²¹ Droplet disruption results depend on the viscosity ratio $\lambda = \eta_d/\eta_c$ between the dispersed phase and the emulsion. The ideal viscosity ratio depends on the flow pattern in the emulsification machine. In general, λ of around 1 is advantageous.^{21,22} The emulsion viscosity is mainly influenced by the continuous-phase viscosity and the dispersed-phase content.²³ In monomeric miniemulsions used for polymerization, both are low. (Inorganic) nanoparticle/monomer suspensions are characterized by increased viscosity and non-Newtonian flow behavior, depending on nanoparticle load and size.²⁴ Thus, extremely high energy inputs, as found only at high pressure and in ultrasonic homogenization, are required.^{25,26}

Ultrasonic miniemulsion homogenization has been well investigated by different research groups.^{16,20,27,28} Here, micelles are avoided by disrupting the droplets (fission) and letting them coalesce (fusion) until the droplet surfaces are sufficiently covered by surfactant molecules for their stabilization and no surfactant molecules are left to form micelles.¹⁹ The process is run until the so-called “steady-state” monomer droplet size distribution is reached, which depends only on the surfactant concentration.¹⁶ Ultrasonic homogenization, however, is critical when dispersed phases with high viscosities have to be dispersed. Often, broad droplet size distributions are found.²⁹ In addition, scaling-up flow cells for continuous production at high throughput proved to be difficult in terms of avoiding bypass flow, abrasion, and product cooling.^{29–31}

High-pressure homogenization is a technical alternative that can be used for the production of miniemulsions on a large scale. The local energy input is comparable to ultrasound application. The main differences are found in the processing time. Droplet disruption and stabilization has to take place within milliseconds,³² which does not allow for a fission–fusion approach as realized in ultrasound homogenization. The droplet stabilization that has to take place at extreme fast kinetics requires working at surfactant concentrations that are high enough.^{33,34}

This may lead to a conflict with the principles of miniemulsion polymerization. In this work, the lower and upper limit of surfactant concentration in MMA miniemulsions was therefore determined for the further process of producing nanoparticle-filled polymer suspensions by high-pressure homogenization.

The surface area covered by one surfactant molecule is characterized by the parameter A_{surf} (eq 1):¹⁶

$$A_{\text{surf}} = \frac{6\varphi M_{\text{SDS}}}{x_{3,2}\rho_{\text{MMA}}C_{\text{SDS}}N_A k} \quad (1)$$

Herein are φ , the dispersed-phase content; M_{SDS} , the molar mass; c_{SDS} , the concentration of SDS; ρ_{MMA} , the density of the monomer; N_A , the Avogadro constant; and k , a correction factor that accounts for the surfactant concentration dissolved in the bulk phase. The Sauter mean diameter $x_{3,2}$ is used to characterize droplet and particle size distributions. This mean diameter characterizes the volume specific surface area of particle collectives and was chosen because interfacial characteristics correlate well with it.³⁵

Two possibilities of droplet disruption have to be considered (Figure 1).

In process route I, energy is applied as long as droplets may disrupt. The droplets are disrupted and coalesce (fission–fusion) until the steady state is reached. The resulting droplet size is determined by the surfactant concentration only because droplets

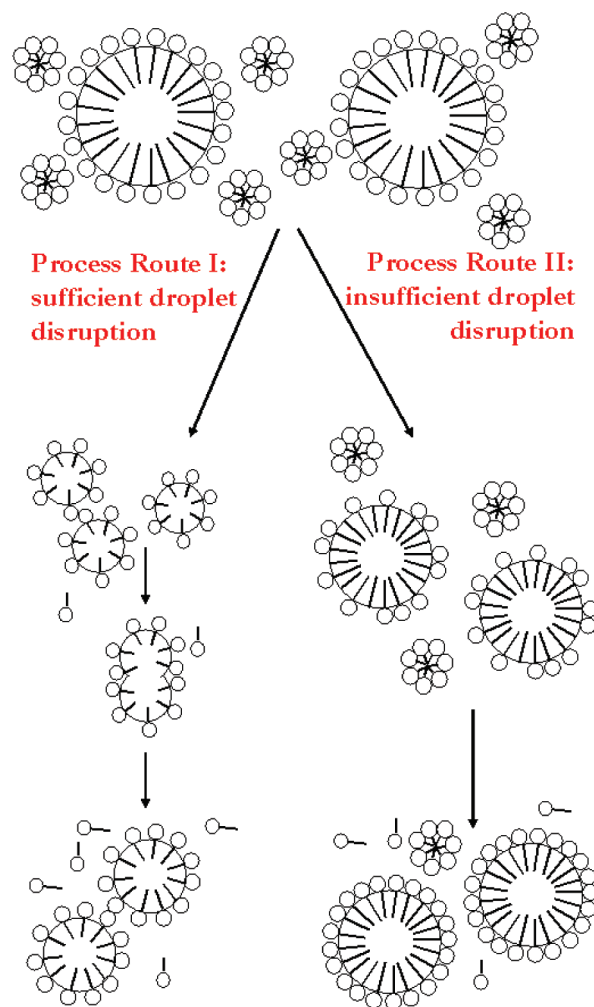


Figure 1. Process routes for droplet breakup (principal scheme).

may be disrupted as long as enough surfactant molecules are left for their stabilization.¹⁶ When the steady state is reached, the surfactant concentration in the bulk phase is low and no micelles are left. The droplet surface area stabilized by one surfactant molecule A_{surf} reaches its highest possible value of $A_{\text{surf,max}}$. For batch-wise ultrasonic homogenization, Landfester et al. reported that the SDS concentration needed to stabilize styrene droplets depends not only on the total surface area in the emulsion at steady state but also on the size of the monomer droplets.¹⁶ This results in a dependence of $A_{\text{surf,max}}$ on the size of the monomer droplets.

In process route II, mechanical energy is applied for a short time only, as found in continuous high-pressure homogenization. The droplet size distribution resulting from this type of processing mainly depends on the mechanical energy input. The steady state is not necessarily reached. That is why the surfactant concentration is higher than in process route I or even micelles can be left in the bulk phase. For miniemulsion polymerization applications, the surfactant concentration has to be adjusted prior to emulsification to ensure that effective surfactant concentration in the continuous phase after homogenization does not lead to micellar or homogeneous nucleation.

The required space of one surfactant molecule in the completely coated interface is given for SDS at 60 nm polystyrene particles: $A_{\text{surf}} \approx 0.5 \text{ nm}^2$. (See, for example, refs 36 and 37.) This value corresponds to the cmc and should therefore be reached before

Table 1. Process Parameters and Surfactant Concentrations Used for Each Droplet Size Interval

droplet size ($x_{3,2}$) interval (nm)	emulsification machines	process parameters	surfactant concentration	surfactant concentration
			(wt % to total mass) during emulsification (%)	(wt % to total mass) during polymerization (%)
0–100	HPH	$\Delta p = 200\text{--}1000$ bar, 0.2 mm valve, continuous process, one passage	0.24–4.8	0.24–4.8
100–200	HPH	$\Delta p = 20$ bar, 0.8 mm valve, continuous process, two passages	0.24	0.24–1.6
200–300	RS, UT	$f = 17\,500\text{--}24\,000$ rpm, batch, $m = 200$ g, $t = 3$ min	0.08–0.24	0.08–0.24
	RS, CM	$f = 10\,000\text{--}12\,000$ rpm, semibatch, $m = 250$ g, $t = 5$ min	0.04	0.04–0.08
400–500	RS, CM	$f = 9000\text{--}10\,000$ rpm, semibatch, $m = 250$ g, $t = 3\text{--}10$ min	0.016–0.08	0.016–0.24

micellar nucleation starts. In this work, we have investigated at which surfactant concentration the regime of miniemulsion polymerization is left and emulsion polymerization starts. The value of A_{surf} at this point has been defined as $A_{\text{surf,min}}$ because it is the minimum occupation of the interface possible in miniemulsion polymerization. At higher surface coverage, micellar or homogeneous nucleation takes place and inhibits a 1:1 copy of droplets to particles. In this work, a method for the calculation of $A_{\text{surf,min}}$ that is dependent on droplet size has been developed.

2. MATERIALS AND METHODS

Materials. Methyl methacrylate was provided by Merck KGaA, hexadecane was purchased from Sigma-Aldrich Inc. (>99%), oil-soluble initiator V59 (2,2-azobis(2-methylbutyronitrile)) was obtained from Wako Chemicals GmbH, and anionic surfactant sodium dodecyl sulfate (SDS) was obtained from Merck KGaA as well as Carl Roth GmbH & Co. KG.

Miniemulsion Formation Methods. For all experiments, a monomer-in-water emulsion with a dispersed phase content of $\varphi = 20$ wt % was produced. To achieve droplet distributions of different sizes, the energy input in emulsification had to be varied over a wide range. Therefore, different emulsification machines and processing parameters had to be used. To achieve small droplet sizes, ultrasonication and high-pressure homogenization (HPH) were used. The instruments used were a Branson (Branson Ultrasonics Corp.) W 450 digital sonifier at 90% amplitude and 0° and a Microfluidics (Microfluidics International Corp.) pump combined with different homogenizing orifice valves with round cross section having different diameters d . (See ref 38 for details of the geometry.) The pressure loss Δp and diameter d are given in Table 1. To achieve defined droplet distributions of a larger size, rotor-stator-emulsifying (RSS) machines had to be applied because at low energy input US and HPH resulted in wide bimodal distributions. As rotor stator systems, a colloid mill (IKA magicLAB (IKA-Werke GmbH & CO. KG)) (RS, ML) and a gear rim dispersing machine (IKA, Ultra-Turrax T25) (RS, UT) were used at varying revolutions f , residence times t , and total masses m , which are given in Table 1. The gap between the rotor and stator of the colloid mill was offset to 0.32 mm.

To investigate process route I and to determine $A_{\text{surf,max}}$ values, miniemulsions with different amounts of surfactant were prepared. A high-energy input was applied for long processing times to achieve the steady-state droplet size distribution depending on the surfactant concentration. Therefore, ultrasonication was used for 120 s in a batch of 50 g. The dispersed phase, consisting of 94.4 wt % MMA, 4 wt % osmotic reagent hexadecane, and 1.6 wt % azo-initiator V59, was mixed with the continuous phase made up of demin water and different amounts (0.016–3.32 wt %) of surfactant SDS. The mixture was stirred for 1 h and then ultrasonicated. The polymerization was carried out overnight at 72°C .

To investigate processing route II, the dispersed phase consisted of 93.8 wt % MMA, 3.9 wt % hexadecane, and 2.3 wt % V59 initiator in all experiments. The polymerization was carried out overnight at 72°C .

To reach different ranges of average droplet sizes that are not dependent on the surfactant concentration, the mechanical energy input was varied by

using the emulsification machines and processing parameters described above. Depending on the droplet size regime investigated, the surfactant concentrations were varied. The material and processing parameters used for each droplet size interval are given in Table 1.

Analytical Methods. The average size and the size distribution of the monomer droplets and the polymer particles were analyzed by means of dynamic light scattering (DLS) at 23°C using a Nicomp particle sizer (model 380, PSS, Santa Barbara, CA) or a Nanotrak (Microtrac, Montgomeryville, PA). Measurements were made with the Nicomp particle sizer at a fixed angle of 90° , and measurements were made with the Nanotrak at 180° .

Measurements of the surface tension γ of the particle suspensions were made with tensiometer DCAT 11 or DCAT 21 from DataPhysics Instruments with the Du Noüy ring method or the Wilhelmy plate method. The radius of the Pt–Ir ring was 4.85 mm, and the wire radius was 0.15 mm. The dimensions of the Pt–Ir plate were $10 \times 19.9 \times 0.2$ mm³.

Transmission electron microscopy (TEM) was carried out with a Zeiss EM902 electron microscope operating at an acceleration voltage of 80 kV. Generally, the samples were prepared by diluting the particle dispersion in demineralized water to about 0.01% solid content; then one droplet of the sample was placed on a 300 mesh carbon-coated copper grid and left to dry overnight at room temperature. Finally, the sample was coated with carbon to protect the polymer in the electron beam.

3. RESULTS AND DISCUSSION

Lower Surfactant Concentration: Avoiding Coalescence during Polymerization. In this work, miniemulsions with rather hydrophilic methyl methacrylate were formed by using different amounts of the SDS surfactant. To reduce secondary particle formation in the continuous phase, hydrophobic initiator V59 was used. To determine the lower surfactant concentration of the miniemulsions, monomer disruption was achieved by ultrasound. The particle diameter, surface tension, and particle surface area per SDS molecule as a function of SDS concentration are shown in Table 2. All values are measured after polymerization. Because the applied surfactant concentration and therefore the surface coverage is very low, the assumption that the droplet size is kept nearly constant during polymerization can be made.¹⁵

The latexes are in size ranges from 49 to 258 nm. In general, a higher amount of surfactant results in a lower surface tension and in a smaller polymer particle size. The size of the particles depends only on the concentration of the SDS, not on ultrasonication power or time. With the used power and time, the steady state is reached and so the size of the droplets is no longer a function of the energy input.¹⁶ The decrease in particle size with increasing amounts of SDS is validated in the TEM images of Figure 2. Sometimes the particles appear to be hollow, but this is only a visual effect of the protection with carbon.

In Figure 3, it is depicted that the value of $A_{\text{surf,max}}$ (calculated with eq 1, assuming $k = 0.8^{39}$) increases with particles size,

Table 2. Variation of the SDS Concentration and Its Influence on Characteristics of the Polymer Latexes

SDS concentration c_{SDS} (wt % to total mass)	particle diameter $x_{3,2}$ (nm)	$A_{\text{surf,max}}$ (nm^2)	surface tension γ ($\text{mN}\cdot\text{m}^{-1}$)	monomer conversion (%)
3.32	49	0.36	35.6	99.98
1.66	64	0.49	36.3	99.25
1.00	68	0.76	38.2	98.33
0.50	77	1.27	46.1	97.23
0.32	81	1.81	50.5	99.25
0.25	85	2.95	53.9	99.89
0.17	93	2.96	56.4	99.74
0.12	101	3.84	60.1	98.39
0.06	154	5.21	61.3	95.45
0.03	195	7.91	61.5	94.34
0.016	258	10.24	64.9	89.90

meaning that the area covered per SDS molecule is larger for large particles.

This may be explained by the droplet collision rate. If emulsions of a given dispersed-phase volume fraction are produced, then the number of resulting droplets depends on their size. When smaller droplets are produced, their number is significantly increased. Because the distance between small droplets is shorter and their number is higher, the collision rate (number of collisions per second) is increased.⁴⁰ Thus, smaller droplets need more protection against coalescence. The value found for $A_{\text{surf,max}}$ is in the range of 0.4–0.5 nm^2 (for mean droplet sizes ranging from 50 to 60 nm), indicating an SDS monolayer or even a multilayer of densely packed surfactant molecules at the droplet surfaces.¹⁶ However, higher values of droplet surface areas stabilized by one surfactant molecule are found for larger droplets (mean size $x > 65$ nm), indicating a less dense packing of the surface with SDS molecules ($A_{\text{surf,max}}$ of up to 10 nm^2). Even then, a fusion–fission rate equilibrium was found, indicating that larger miniemulsion droplets tolerate incomplete coverage without coalescing.

Surface tension measurements of the latex suspensions are given in Table 2 and Figure 5. They range from 36 to 65 $\text{mN}\cdot\text{m}^{-1}$ and decrease with decreasing particle size. This supports the hypothesis of incomplete surface coverage at increased particle size because there is an equilibrium among the surfactant molecules dissolved, those adsorbed at particle interfaces, and those adsorbed at the polymer suspension/air surface.¹⁶

The results depict that with MMA as the monomer there is a dependency of $A_{\text{surf,max}}$ on the size of the monomer droplets of an MMA-in-water miniemulsion as already found for styrene.¹⁶ The $A_{\text{surf,max}}$ values correspond to the surfactant concentrations that are necessary to stabilize a certain droplet size against coalescence. They are therefore the maximum surface areas (depending on droplet size) that can be stabilized by one surfactant molecule without leading to an increase in droplet size. With decreasing amounts of surfactant, the miniemulsion does not necessarily become unstable but the achievable particle size will increase.

Upper Surfactant Concentration Limit: Avoiding Emulsion Polymerization. However, the surfactant concentration cannot be increased to any amount. Once micelles are formed, there is a risk of the polymerization following the emulsion polymerization principle, which would not allow for keeping the droplet inner structure. To identify the maximum surfactant concentration that results in an emulsion polymerization,

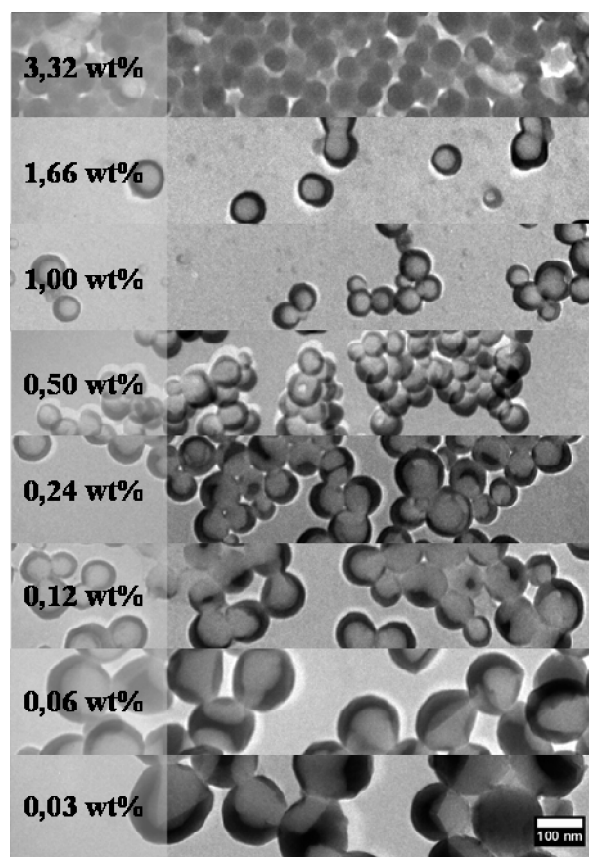


Figure 2. TEM images of PMMA particles after batchwise ultrasonification at given SDS concentrations (from 0.03 to 3.32 wt % SDS to total mass), followed by miniemulsion polymerization (Table 2). The particles are protected by carbon.

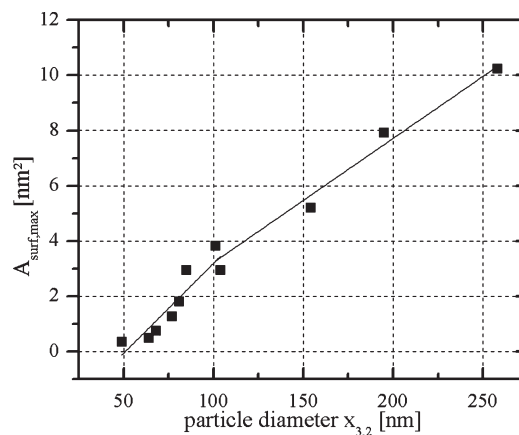


Figure 3. Maximal surface area stabilized by one SDS molecule ($A_{\text{surf,max}}$ values) vs the Sauter mean diameter.

MMA-in-water miniemulsions were produced by varying the SDS concentration and the mechanical energy input by using different emulsification machines (Table 1). The droplet size distribution before polymerization and the particle size distribution after polymerization were measured by dynamic light scattering. A change in the Sauter mean diameter $\Delta x_{3,2}$ during polymerization indicates the polymerization type: In miniemulsion polymerization, droplet sizes are equal to

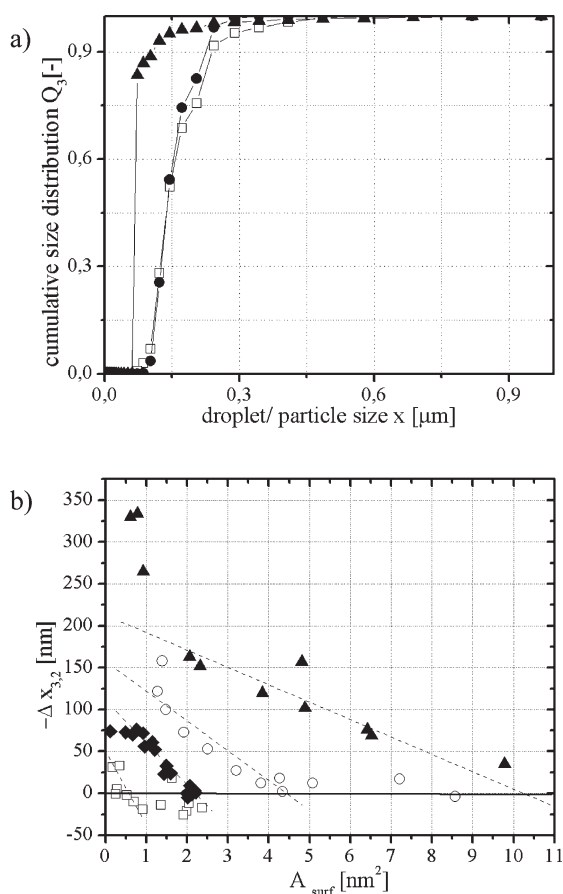


Figure 4. (a) (□) Droplet size distribution of a monomer emulsion before polymerization and a particle size distribution after polymerization ((●) $c_{\text{sds}} = 0.24\%$ and $A_{\text{surf}} = 2.2 \text{ nm}^2$; (▲) $c_{\text{sds}} = 0.67\%$ and $A_{\text{surf}} = 0.7 \text{ nm}^2$). (b) Decrease in particle size after polymerization depending on the monomer droplet surface area stabilized by SDS molecules (A_{surf}) for monomer droplets of different size ranges ((□) $x_{3,2} \leq 100 \text{ nm}$; (◆) $100 \text{ nm} < x_{3,2} \leq 200 \text{ nm}$; (○) $200 \text{ nm} < x_{3,2} \leq 300 \text{ nm}$; (▲) $400 \text{ nm} < x_{3,2} \leq 500 \text{ nm}$).

particle sizes (1:1 transfer). In emulsion polymerization, polymers are formed within micelles or by homogeneous nucleation. The resulting particles are significantly smaller than the monomer droplets, which serve only as a monomer reservoir. In Figure 4a, the change in the particle size distribution is shown for two different surfactant concentrations at a droplet size of $x_{3,2} \approx 150 \text{ nm}$. The unfilled symbols show the droplet size distribution before polymerization, and the filled symbols show the distributions after polymerization. At a value of $A_{\text{surf}} = 2.2 \text{ nm}^2$, the droplet/particle size is nearly constant throughout the polymerization whereas for a lower A_{surf} there is a significant decrease in droplet/particle size. The difference between droplet size before polymerization and particle size after polymerization $\Delta x_{3,2}$ will be used for further calculations. In Figure 4b, the decrease in the Sauter mean diameter $-\Delta x_{3,2}$ depending on the value of A_{surf} for different ranges of the average droplet size $x_{3,2}$ is plotted. To achieve different ranges of droplet size, it was necessary to use different emulsifying machines with varying process parameters; for details, see Table 1. The droplet size before polymerization therefore did not depend on the surfactant concentration. A_{surf} was calculated according to eq 1.

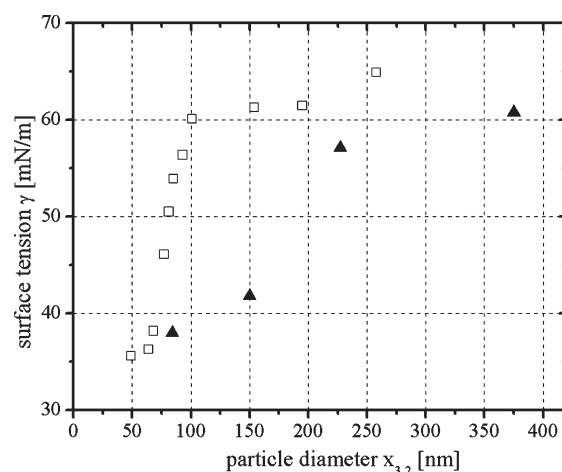


Figure 5. Surface tension γ vs particle diameter after polymerization at (□) $A_{\text{surf,max}}$ and (▲) $A_{\text{surf,min}}$.

In Figure 4b, it can be clearly seen that miniemulsion polymerization of the MMA monomer can be realized only at values of A_{surf} that are high enough. With decreasing values of A_{surf} , the Sauter mean diameter difference increases, indicating a higher percentage of polymer particles produced by emulsion polymerization processes such as micellar and homogeneous nucleation.

The intersection with the x axis ($\Delta x_{3,2} = 0 \text{ nm}$) of the best-fitting curve gives the value of $A_{\text{surf,min}}$ because no difference between monomer droplet and polymer particle size after polymerization could be detected here. As already found for $A_{\text{surf,max}}$, the values of $A_{\text{surf,min}}$ also depend on the monomer droplet size. The larger the droplets, the larger the surface area that is occupied by one SDS molecule at the starting point of an emulsion polymerization. Consecutively, the values of $A_{\text{surf,min}}$ are higher than the $A_{\text{surf,min}} = 0.5 \text{ nm}^2$ value found in the literature for droplets larger than 100 nm .

The polymer suspension/air surface tension as a function of polymer particle size after miniemulsion polymerization is given in Figure 5. The surface tension increases with particle size because the surfactant concentration used is lower for larger droplets. The value of the surface tension of the emulsions prepared with the maximum surfactant concentration possible in miniemulsion polymerization ($A_{\text{surf,min}}$) is lower than the surface tension of the suspensions prepared with a minimum surfactant concentration ($A_{\text{surf,max}}$). This is valid for all particle sizes. There is an equilibrium among the surfactant molecules adsorbed at the surface of the suspension, those dissolved in the continuous phase, and those adsorbed at the particle interface.¹⁶ Therefore, the data in Figure 5 supports the assumption that more surfactant is adsorbed at the particle interface at the maximum surfactant concentration applicable ($A_{\text{surf,min}}$) than at the minimum surfactant concentration necessary ($A_{\text{surf,max}}$) because the interfacial tension is lower in the first case. However, the interfacial tension is higher than the value at the cmc of about $32 \text{ mN} \cdot \text{m}^{-1}$, indicating the absence of micelles in the bulk phase.

In Figure 6, $A_{\text{surf,max}}$ and $A_{\text{surf,min}}$ values are given depending on $x_{3,2}$. $A_{\text{surf,min}}$ is always smaller than $A_{\text{surf,max}}$. This means that more surfactant molecules per area can adsorb at the interface than are needed for the critical stabilization but the interface is not completely covered with surfactant. Like $A_{\text{surf,max}}$, $A_{\text{surf,min}}$

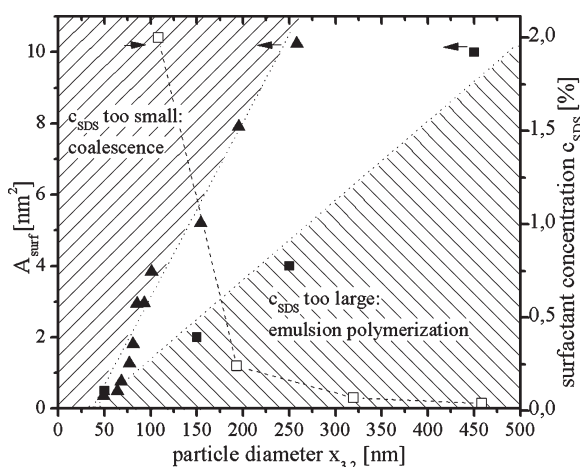


Figure 6. Comparison of $A_{\text{surf,min}}$ and $A_{\text{surf,max}}$ and the maximum surfactant concentration (wt % to total mass) being applicable without leading to emulsion polymerization (with monomer diffusion) for $\varphi = 20\%$ depending on droplet size.

also depends on the droplet size. However, this cannot be explained by the collision rate depending on droplet diameter because more surfactant is adsorbed at the interfaces than is required for stabilization.

Most likely the mechanism responsible for the decrease in size during polymerization is found in homogeneous nucleation. Huang et al. found that increasing the surfactant concentration but keeping it below the cmc led to a decrease in polymer particle size. They explain it by an increase in homogeneous nucleation, hypothesizing that more surfactant molecules were available for the stabilization of the precipitated oligomers.⁴¹ However, the authors do not give the corresponding droplet size distribution before polymerization, so it is not conclusive. Also, this does not explain the increase in $A_{\text{surf,min}}$ with droplet size.

At constant surfactant concentration, the homogeneous nucleation rate increases with increasing droplet size; as the number of droplets is reduced, so is the probability of the oligomers being captured by a droplet before precipitation.^{42,43}

Those approaches can be combined to explain the fact that miniemulsion polymerization can be run at lower surfactant concentrations in the larger droplet size regime. At a constant droplet phase volume, the number of droplets decreases with increasing droplet size. Thus, the surfactant concentration has to decrease to keep the probability for homogeneous nucleation constant. The surfactant concentrations at $A_{\text{surf,min}}(x_{3,2})$ were used for the calculation of the ratio of the surfactant molecules in the emulsion (N_{SDS}) to the number of droplets (N_{droplet}). It was striking that the value of the ratio was nearly constant for all droplet sizes examined: $N_{\text{SDS}}/N_{\text{droplet}} = 45\,000$.

This in turn leads to the conclusion that the surfactant concentration in the continuous phase after emulsification not only has to be lower than the cmc to avoid micellar nucleation but also has to be adjusted to even lower surfactant concentrations depending on the number of droplets in order to reduce homogeneous nucleation processes. Once a certain ratio of the number of surfactant molecules to the number of droplets is exceeded, a massive increase in homogeneous nucleation is found.

Regarding the processing of monomer miniemulsions, this fact limits the possibility of using the miniemulsion polymerization processing principle for the production of polymer latexes. Even

though $A_{\text{surf,min}}$ is smaller than $A_{\text{surf,max}}$, the increasing value of $A_{\text{surf,min}}$ with droplet size leads to surfactant concentrations allowed within the continuous phase being quite low (Figure 6). Nonetheless, a knowledge of $A_{\text{surf,min}}$ and $A_{\text{surf,max}}$ values allows for calculating the correct surfactant concentration regime depending on the target droplet or polymer particle size. For $A_{\text{surf}} > A_{\text{surf,max}}$, droplets will coalesce and droplet and particle sizes will increase. This may not lead to complete destabilization of the emulsion but to an increase in droplet size, which is also an undesired effect. For $A_{\text{surf}} < A_{\text{surf,min}}$, the polymerization process will follow the emulsion polymerization principle, leading to significantly lower particle sizes and a loss of their inner structure. The latter cannot be accepted in the production of core-shell nanoparticles. The surfactant concentration has to be well adapted to keep $A_{\text{surf,min}} \leq A_{\text{surf}} \leq A_{\text{surf,max}}$ in order to produce a stable miniemulsion and a polymer latex of the desired particle size and structure.

4. CONCLUSIONS

In batchwise ultrasonication, monomer droplet and resulting polymer particle sizes are determined by the surfactant concentration. By knowing the particle size, the dispersed-phase content, and the amount of SDS applied, the interfacial area that can be stabilized per one surfactant molecule $A_{\text{surf,max}}$ can be calculated. Smaller particles have a densely covered surface ($A_{\text{surf,max}} \approx 0.4 \text{ nm}^2$) whereas larger particles are stabilized even when being only partially capped ($A_{\text{surf,max}} \approx 10 \text{ nm}^2$).

In continuous miniemulsion production (e.g. by high-pressure homogenization), in order to obtain a high-volume production rate, the surfactant concentration has to be intelligently adapted. It is important to use surfactant concentrations that are high enough to guarantee an adequate stabilization of the droplets in a short time. However, surfactant concentrations in the continuous phase have to be lower than the cmc to avoid micellar nucleation. In this work, it was found that this is not the only limit for the upper surfactant concentration. In addition, the surfactant concentration has to be reduced to values lower than the cmc to avoid homogeneous nucleation in the bulk phase. Corresponding to this concentration, there is a minimum monomer droplet surface area that has to be occupied by one surfactant molecule $A_{\text{surf,min}}$. As expected, $A_{\text{surf,min}}$ was found to be higher than $A_{\text{surf,max}}$. The ratio of the number of surfactant molecules in the emulsion to the number of monomer droplets seems to have a significant influence on the rate of homogeneous nucleation during polymerization. With a knowledge of $A_{\text{surf,max}}$ and $A_{\text{surf,min}}$, the required surfactant concentration for target particle sizes can be calculated and used for the successful production of polymer particles by the miniemulsification technique. Therefore, PMMA particles of different sizes can be synthesized in continuous production by high-pressure homogenization at volume flow rates of up to several thousand liters per hour.

■ AUTHOR INFORMATION

Corresponding Author

*E-mail: lena.hecht@kit.edu. Tel: +49 721 608 43614. Fax: +49 721 45967.

■ ACKNOWLEDGMENT

This project was funded by the German Research Foundation (SPP1273).

REFERENCES

- (1) Landfester, K. *Annu. Rev. Mater. Res.* **2006**, *36*, 231–279.
- (2) Landfester, K. *Angew. Chem., Int. Ed.* **2009**, *48*, 4488–4507.
- (3) Tiarks, F.; Landfester, K.; Anonietti, M. *Macromol. Chem. Phys.* **2001**, *202*, 51–60.
- (4) Steiert, N.; Landfester, K. *Macromol. Mater. Eng.* **2007**, *292*, 1111–1125.
- (5) Theisinger, S.; Schoeller, K.; Osborn, B.; Sarkar, M.; Landfester, K. *Macromol. Chem. Phys.* **2009**, *210*, 411–420.
- (6) Volz, M.; Walther, P.; Ziener, U.; Landfester, K. *Macromol. Mater. Eng.* **2007**, *292*, 1237–1244.
- (7) Erdem, B.; Sudol, E. D.; Dimonie, V. L.; El-Aasser, M. S. *J. Polym. Sci., Part A: Polym. Chem.* **2000**, *38*, 4419–4430.
- (8) Jordan, A.; Wust, P.; Scholz, R.; Tesche, B.; Föhling, H.; Mitrovics, T.; Vogl, T.; Cervós-Navarro, J.; Felix, R. *Int. J. Hyperther.* **1996**, *12*, 705–722.
- (9) Weiss, C. K.; Lorenz, M. R.; Landfester, K.; Mailänder, V. *Macromol. Biosci.* **2007**, *7*, 883–896.
- (10) Bechthold, N.; Tiarks, F.; Willert, M.; Landfester, K.; Antonietti, M. *Macromol. Symp.* **2000**, *151*, 549–555.
- (11) Erdem, B.; Sudol, E. D.; Dimonie, V. L.; El-Aasser, M. S. *J. Polym. Sci., Part A: Polym. Chem.* **2000**, *38*, 4431–4440.
- (12) Hoffmann, D.; Landfester, K.; Antonietti, M. *Magnetohydrodynamics* **2001**, *37*, 217–221.
- (13) Zhang, S. W.; Zhou, S. X.; Weng, Y. M.; Wu, L. M. *Langmuir* **2005**, *21*, 2124–2128.
- (14) Antonietti, M.; Landfester, K. *Prog. Polym. Sci.* **2002**, *27*, 689–757.
- (15) Landfester, K.; Bechthold, N.; Foerster, S.; Antonietti, M. *Macromol. Rapid Commun.* **1999**, *20*, 81–84.
- (16) Landfester, K.; Bechthold, N.; Tiarks, F.; Antonietti, M. *Macromolecules* **1999**, *32*, 5222–5228.
- (17) Asua, J. M. *Prog. Polym. Sci.* **2002**, *27*, 1283–1346.
- (18) Luo, Y. W.; Schork, F. J. *J. Polym. Sci., Part A: Polym. Chem.* **2002**, *40*, 3200–3211.
- (19) Landfester, K. *Adv. Mater.* **2001**, *13*, 765–768.
- (20) Ouzineb, K.; Lord, C.; Lesauze, N.; Graillat, C.; Tanguy, P. A.; McKenna, T. *Chem. Eng. Sci.* **2006**, *61*, 2994–3000.
- (21) Schuchmann, H. P. In *Product Design and Engineering: Best Practices*; Bröckel, U., Meier, W., Wagner, G., Eds.; Wiley-VCH: Weinheim, Germany, 2007.
- (22) Grace, H. P. *Chem. Eng. Commun.* **1982**, *14*, 225–277.
- (23) Windhab, E. J. In *Emulgiertechnik*; Schubert, H., Ed.; Behr's Verlag: Hamburg, 2005.
- (24) Pahl, M.; Gleissle, W.; Laun, H. M. *Praktische Rheologie der Kunststoffe und Elastomere*; VDI-Verlag: Düsseldorf, 1991.
- (25) Abismail, B.; Canselier, J. P.; Wilhelm, A. M.; Gourdon, C. *Ultrason. Sonochem.* **1999**, *6*, 75–83.
- (26) Landfester, K. *Macromol. Rapid Commun.* **2001**, *22*, 896–936.
- (27) Fontenot, K.; Schork, F. J. *J. Appl. Polym. Sci.* **1993**, *49*, 633–655.
- (28) Rodriguez, V. S.; Elaasser, M. S.; Asua, J. M.; Silebi, C. A. *J. Polym. Sci., Part A: Polym. Chem.* **1989**, *27*, 3659–3671.
- (29) Bechtel, S.; Gilbert, N.; Wagner, H. G. *Chem. Ing. Tech.* **2000**, *72*, 450–459.
- (30) Behrend, O.; Schubert, H. *Partec 2001, International Congress for Particle Technology*, Nürnberg, 2001.
- (31) Kentish, S.; Wooster, J.; Ashokkumar, A.; Balachandran, S.; Mawson, R.; Simons, L. *Innovative Food Sci. Emerg. Technol.* **2008**, *9*, 170–175.
- (32) Stang, M.; Karbstein, H.; Schubert, H. *Chem. Eng. Process.* **1994**, *33*, 307–311.
- (33) Stang, M. *Zerkleinern und Stabilisieren von Tropfen beim mechanischen Emulgieren*. Ph.D. Dissertation, University of Karlsruhe (TH), 1998.
- (34) Tcholakova, S.; Denkov, N. D.; Danner, T. *Langmuir* **2004**, *20*, 7444–7458.
- (35) Merkus, H. G. *Particle Size Measurements: Fundamentals, Practice, Quality*; Springer: Heidelberg, 2009.
- (36) Nodehi, A.; Moosavian, M. A.; Haghighi, M. N.; Sadr, A. *Chem. Eng. Technol.* **2007**, *30*, 1732–1738.
- (37) Piirma, I.; Chen, S. R. *J. Colloid Interface Sci.* **1980**, *74*, 90–102.
- (38) Aguilar, F. A.; Köhler, K.; Schubert, H.; Schuchmann, H. P. *Chem. Ing. Tech.* **2008**, *80*, 607–613.
- (39) Bechthold, N. *Polymerisation in Miniemulsion*. Ph.D. Dissertation, University of Potsdam, 2000.
- (40) Chesters, A. K. *Chem. Eng. Res. Des.* **1991**, *69*, 259–270.
- (41) Huang, H.; Zhang, H. T.; Li, J. Z.; Cheng, S. Y.; Hu, F.; Tan, B. *J. Appl. Polym. Sci.* **1998**, *68*, 2029–2039.
- (42) Rodriguez, R.; Barandiaran, M. J.; Asua, J. M. *Macromolecules* **2007**, *40*, 5735–5742.
- (43) Ferguson, C. J.; Russell, G. T.; Gilbert, R. G. *Polymer* **2002**, *43*, 4557–4570.